

---

# JOURNAL OF THE AMERICAN CHEMICAL SOCIETY

---

## Chemistry of Nitric Oxide with Protein-Bound Iron Sulfur Centers. Insights on Physiological Reactivity

Matthew W. Foster and J. A. Cowan\*

Contribution from Evans Laboratory of Chemistry, The Ohio State University, 100 West 18th Avenue,  
Columbus, Ohio 43210.

Received January 11, 1999

**Abstract:** The anaerobic reaction of *C. vinosum* high-potential iron protein (HiPIP) with nitric oxide has been studied in order to understand the chemical reactivity of NO with protein-bound iron–sulfur clusters. Despite having a solvent inaccessible 4Fe–4S center, native HiPIP reacts with diethylamineNONOate (an NO donor), resulting in protein unfolding and the formation of protein-bound dinitrosyl–iron complexes (DNICs) with a typical  $g_{av} = 2.03$  EPR signal. These cysteinyl-coordinated DNICs are directly observed for the first time by use of electrospray ionization–mass spectrometry (ESI-MS) and are found only in a stoichiometry of 2:1 DNIC:protein. Our results suggest that these complexes form only when the protein is folded. ESI-MS also demonstrates that NO-mediated cluster degradation results in nitrosation of the protein at sites other than cysteine. Finally, reactivity comparison of native and Tyr19Leu HiPIP demonstrates solvent accessibility to be an important, but not necessary factor for Fe–S cluster degradation by NO. By use of UV–visible, NMR, and EPR spectroscopies, as well as ESI-MS, we have determined the major products of degradation and elucidate some of the mechanistic issues governing cluster degradation, protein nitrosation, and DNIC formation. Comparisons are made between the nitric oxide chemistry of bacterial HiPIP and other eukaryotic and prokaryotic iron–sulfur proteins that are relevant in vivo targets for NO.

### Introduction

Nitric oxide serves diverse roles in biology: it affects proteins that regulate gene transcription and translation, acts as a secondary messenger in signaling pathways, and is a cytotoxic agent.<sup>1</sup> The primary targets for NO are metal-containing proteins; however, the products of its reaction with dioxygen ( $\text{NO}_x$ ), superoxide ( $\text{ONOO}^-$ ), and transition metals ( $\text{NO}^+$ , M–NO) are observed to react with nucleic acids, amino acid side chains, and a variety of low molecular weight amines and thiols.<sup>1,2</sup>

The formation of a  $g_{av} = 2.03$  EPR signal characteristic of  $[\text{L}_2\text{Fe}(\text{NO})_2]^-$ , a  $d^7$  dinitrosyl–iron(I) complex (DNIC), is a biological marker of NO-mediated degradation of iron–sulfur proteins. For the most part, DNICs and iron–sulfur clusters share the same ligands (namely cysteine thiolates), although dinitrosyl–iron complexes containing a wide range of O/N/S ligation have been observed.<sup>3–6</sup> Cysteinyl coordination of protein-bound DNICs has been shown solely by comparison of protein-derived  $g_{av} = 2.03$  EPR signals to those of small-molecule dinitrosyl–iron complexes.<sup>7</sup>  $[(\text{Cys})_2\text{Fe}(\text{NO})_2]^-$  has

(1) Stamler, J. S. *Cell* **1994**, 78, 931–936.

(2) Radi, R. *Chem. Res. Toxicol.* **1995**, 9, 828–835.

(3) Boese, M.; Mordvintsev, P. I.; Vanin, A. F.; Busse, R.; Mulsch, A. *J. Biol. Chem.* **1995**, 270, 29244–29249.

(4) Branca, M.; Culeddu, N.; Fruianu, M.; Marchettini, N.; Tiezzi, E. *Magn. Reson. Chem.* **1997**, 35, 687–690.

(5) Lee, M.; Arosio, P.; Cozzi, A.; Chasteen, N. D. *Biochemistry* **1994**, 33, 3679–3687.

(6) McDonald, C. C.; Phillips, W. D.; Mower, H. F. *J. Am. Chem. Soc.* **1965**, 87, 3319–3326.

(7) Butler, A. R.; Glidewell, C.; Li, M.-H. *Adv. Inorg. Chem.* **1988**, 32, 335–393.

been structurally characterized by EPR by virtue of the hyperfine splitting that arises from  $^{15}\text{NO}$  or  $^{14}\text{NO}$  and the  $\beta\text{-CH}_2$  protons of cysteine, for example.<sup>6</sup>

The degradation of iron–sulfur proteins to form DNICs is now well documented. In particular, Reddy et al. have shown that treatment of intact cells of *Clostridium botulinum* with sodium nitrite resulted in formation of a  $g_{\text{av}} = 2.03$  signal.<sup>8</sup> Furthermore, after treatment with  $\text{NaNO}_2$ /ascorbate, a source of nitric oxide, the  $g = 1.94$  EPR signal arising from *C. botulinum* iron–sulfur proteins was lost, and the observed  $g_{\text{av}} = 2.03$  signal was significantly more intense. This study suggested that degradation of important iron–sulfur proteins was the basis for the antimicrobial activity of nitrite in cured food.<sup>9</sup> In addition, nitric oxide synthesized by macrophages has also been shown to differentially inhibit several mitochondrial proteins that contain iron–sulfur centers.<sup>10,11</sup>

Most recently, attention has focused on the reaction of NO and peroxynitrite ( $\text{ONOO}^-$ ) with the iron regulatory protein (IRP1) and related mitochondrial aconitases.<sup>12–14</sup> IRP1 contains a 4Fe–4S cluster and exhibits aconitase activity. The cluster can undergo oxidation to an inactive 3Fe–4S form and can be completely degraded to apo-IRP1.<sup>15</sup> Apo-IRP1 plays a role in iron homeostasis by binding to iron regulatory elements (IREs) contained in the 3'- and 5'-untranslated region of some mRNA's. By this mechanism, IRP1 can inhibit translation of the iron-storage protein ferritin, but activate translation of the transferrin-receptor protein.<sup>16</sup> Nitric oxide provides a plausible mechanism for conversion of IRP1 from its Fe–S cluster-containing form to the RNA-binding form. Recently, it has been shown that the reaction of NO, both with the IRP1 and mitochondrial aconitase, results in the formation of protein-bound DNICs.<sup>13</sup>

Nitrosylation of cysteine is an important regulatory mechanism *in vivo*.<sup>1</sup> The formation of Cys-NO (RS–NO for any thiol) occurs via the nitrosating agent  $\text{NO}^+$ , which requires an electron acceptor such as iron to oxidize NO. Alternatively, nitrosylation can occur via transnitrosation by a low molecular weight S-nitrosothiol.<sup>1</sup> The formation of N-nitrosamines and N-nitrosamides by similar mechanisms is not known to play any regulatory role *in vivo*, but these compounds are known carcinogens, and N-nitrosamines have been studied with respect to their ability to cause deamination and mutagenesis.<sup>17</sup> In fact, under the mildly acidic environments of mammalian stomachs, nitrosation of peptides by nitrite (or more likely nitrous acid) is known to occur. Thus, N-nitrosamine formation may explain the correlation between nitrite and/or protein intake and dietary-related cancer.<sup>9</sup> There are few reports of N-nitrosation of proteins at physiological pH, and most model studies have been carried out in organic solvents using  $\text{N}_2\text{O}_4(\text{g})$ , or in aqueous acidic (0.5 M HCl) solutions of  $\text{NaNO}_2$ .<sup>17–19</sup> Recently, the aerobic reaction

of peptide angiotensin II with NO at pH 7.4 has been shown by mass spectrometry to result in degradation of the arginine side chain via N-nitroso intermediates.<sup>20</sup>

In this paper we report experiments designed to elucidate the chemistry of nitric oxide with a prototypical Fe–S cluster-containing protein, namely, the high potential iron protein (HiPIP) from *Chromatium vinosum*. In particular, we directly determine the extent of DNIC formation by electrospray ionization–mass spectrometry (ESI-MS) as well as observe nitrosation/nitrosylation of the protein itself. Our results suggest that the formation of protein-bound DNICs reflects the state of protein folding and depends on the mechanism of cluster degradation. By use of known structure–reactivity relationships of native and Tyr19Leu HiPIP we demonstrate that solvent accessibility of the iron–sulfur cluster is an important factor in determining its reactivity with NO. The results obtained herein provide insight on some of the aforementioned examples of NO reactivity with biological targets.

## Experimental Methods

**Protein preparation.** Recombinant reduced native and Tyr19Leu *C. vinosum* HiPIPs (including uniformly  $^{15}\text{N}$ -labeled) were isolated and purified as described previously.<sup>21,22</sup> Apo-HiPIP was prepared by acid-degradation of the  $\text{Fe}_4\text{S}_4$  cluster with 0.5 M HCl in the presence of 5 M guanidine hydrochloride,<sup>23</sup> followed by extensive dialysis (against Tris-HCl pH 8, 2 mM EDTA, 5 mM 2-mercaptoethanol) and finally by exchange into 50 mM Hepes, pH 7.4. HiPIP was oxidized by reaction with a 10-fold excess of potassium ferricyanide.

**Nitric Oxide Sources.** The NO donor, diethylamineNONOate (DEANO), was chiefly used since it could rapidly deliver the high concentrations (millimolar) of NO required for NMR and ESI-MS studies. DEANO was purchased from Cayman Chemical Co. (Ann Arbor, MI.). Stock solutions of the NONOates were prepared anaerobically in 10 mM NaOH and were stored at  $-80^\circ\text{C}$ . Concentrations were verified from extinction coefficients supplied by the manufacturer for diethylamineNONOate ( $\epsilon = 6500 \text{ M}^{-1} \text{ cm}^{-1}$  at 250 nm). The  $t_{1/2}$  for NONOate decomposition was determined by monitoring the change in absorbance of DEANO at 250 nm. At room temperature in 50 mM Hepes, pH 7.4, the  $t_{1/2}$  of DEANO was found to be  $\sim 8$  min. Alternatively, NO-saturated solutions were prepared by bubbling NO gas (Liquid Carbonic) through deaerated 5 M NaOH and into Ar-purged water.

**Sample Preparation.** Typically, HiPIP ( $\sim 50 \mu\text{M}$  for UV–vis and certain EPR experiments;  $\sim 1 \text{ mM}$  for EPR, NMR, and ESI-MS experiments) in 50 mM Hepes, pH 7.4, was deaerated by successive pump/purge cycles using a house vacuum and purified argon. A concentrated solution (100 to 500 mM) of DEANO was added to the protein via a gastight Hamilton syringe to give the appropriate excess of NONOate. Unless otherwise noted, samples were reacted at room temperature for 1 h and stored at  $-80^\circ\text{C}$ . For the reaction of apo-HiPIP with  $\text{FeSO}_4$  and DEANO, apo-HiPIP was first incubated anaerobically with a 20-fold excess of 2-mercaptoethanol for 10 min and subsequently desalted on a G-25 column equilibrated with Ar-purged buffer. The dinitrosyl–iron complex of cysteine,  $[\text{Fe}(\text{Cys})_2(\text{NO})_2]^-$ , was synthesized from  $\text{FeSO}_4$ ,  $\text{NaNO}_2$ , and cysteine as described previously.<sup>4</sup>

**UV–Visible Spectroscopy.** Reactions were monitored with a Hewlett-Packard 8425A diode array spectrophotometer using the On-

(8) Reddy, D.; Lancaster, J. R.; Cornforth, D. P. *Science* **1983**, *221*, 769–770.

(9) Challis, B. C.; Milligan, J. R.; Mitchell, R. C. *J. Chem. Soc., Chem. Commun.* **1984**, 1050–1051.

(10) Drapier, J.-C.; Hibbs, J. B. *J. Clin. Invest.* **1986**, *78*, 790–797.

(11) Drapier, J.-C. *Methods* **1997**, *11*, 319–329.

(12) Bouton, C.; Hirling, H.; Drapier, J.-C. *J. Biol. Chem.* **1997**, *272*, 19969–19975.

(13) Kennedy, M. C.; Antholine, W. E.; Beinert, H. *J. Biol. Chem.* **1997**, *272*, 20340–20347.

(14) Gardner, P. R.; Costantino, G.; Szabo, C.; Salzman, A. L. *J. Biol. Chem.* **1997**, *272*, 25071–25076.

(15) Beinert, H.; Kennedy, M. C.; Stout, C. D. *Chem. Rev.* **1996**, *96*, 2335–2373.

(16) Hentze, M. W.; Kuhn, L. C. *Proc. Natl. Acad. Sci. U.S.A.* **1996**, *93*, 8175–8182.

(17) Paik, S.; White, E. H. *Tetrahedron Lett.* **1994**, *35*, 7731–7734.

(18) Bonnet, R.; Hollyhead, R.; Johnson, B. L.; Randall, E. W. *J. Chem. Soc., Perkin Trans. 1* **1975**, 2261–2264.

(19) Challis, B. C.; Milligan, J. R.; Mitchell, R. C. *J. Chem. Soc., Perkin Trans. 1* **1990**, 3103–3108.

(20) Ducrocq, C.; Dendane, M.; Laprevote, O.; Serani, L.; Das, B. C.; Bouchemal-Chibani, N.; Doan, B.-T.; Gillet, B.; Karim, A.; Carayon, A.; Payen, D. *Eur. J. Biochem.* **1998**, *253*, 146–153.

(21) Agarwal, A.; Tan, J.; Eren, M.; Tevelev, A.; Lui, S. M.; Cowan, J. A. *Biochem. Biophys. Res. Commun.* **1993**, *197*, 1357–1362.

(22) Agarwal, A.; Li, D.; Cowan, J. A. *Proc. Natl. Acad. Sci. U.S.A.* **1995**, *92*, 9440–9444.

(23) Moulis, J.-M.; Lutz, M.; Gaillard, J.; Noodleman, L. *Biochemistry* **1988**, *27*, 8712–8719.

Line Instrument Systems (OLIS) 4300S Operating System software. Protein solutions (typically 30–50  $\mu\text{M}$  in a volume of 700  $\mu\text{L}$ ) were purged with argon in a septum-sealed quartz cuvette (0.7 cm  $\times$  0.7 cm) prior to addition of the NONOate. Spectra were recorded over the range of 230 to 700 nm for timed scans or at 350 nm for time-drive experiments.

**EPR Spectroscopy.** EPR spectra were recorded with an X-band Bruker ESP 300 spectrometer equipped with an Oxford liquid helium cryostat. Samples were frozen in dry ice/acetone and stored at 77 K. Low-temperature EPR spectra were taken under the following conditions: microwave power and frequency, 0.1 mW and 9.45 GHz; modulation amplitude and frequency, 5.054 G and 100 kHz; time constant, 10.24 ms; and temperature, 15 K. Room temperature spectra were recorded in a flat cell under similar conditions, with the following changes: microwave frequency, 9.66 GHz; and modulation amplitude, 0.56 G for cysteine complexes, and 5.06 G for protein samples. The  $S = 1/2$  signal of ferricyanide-oxidized HiPIP was used as a standard for spin integrations.

**NMR Spectroscopy.**  $^1\text{H}$ – $^{15}\text{N}$  HSQC spectra were acquired on a Bruker 600 Avance spectrometer operating at 600.13 MHz and 298 K. HSQC experiments were acquired in the States-TPPI mode, including receiver inversion, using an HSQC program with water flip back and WATERGATE for water suppression.<sup>24,25</sup> Spectra were acquired in a DQD mode with 128 transients using a relaxation delay of 1.2 ms, and were processed using Bruker's XWINNMR software. NMR samples contained 10% (v/v)  $\text{D}_2\text{O}$  which was added prior to reaction with DEANO. After reaction with NONOates, samples were subsequently transferred anaerobically to septum-sealed NMR tubes using a gastight Hamilton syringe.

**Liquid Chromatography ESI–Mass Spectrometry.** Prior to LC-ESI-MS analysis, samples were desalted on a G-25 column to remove any NONOate or other  $\text{NO}_x$  species (nitrate, nitrite, etc.) that could cause further chemistry to the protein under acidic conditions. Samples were passed through a Shimadzu LC-10AD HPLC with a Deltabond C8 column (2  $\times$  150 mm) before direct injection into the ESI-MS. Typically, 10  $\mu\text{L}$  of a 3 mg/mL (0.3 mM) sample was injected and, with a flow rate of 0.2 mL/min, washed with 100% buffer A for 3 min and eluted with a linear gradient of 0–90% buffer B for 15 min. Buffer A contained 0.1% TFA (v/v) in water, and buffer B contained 0.05% (v/v) TFA in acetonitrile. MS analysis was carried out on a Perkin-Elmer Sciex API 300 triple quadrupole mass spectrometer operating in the positive ion mode. Mass spectra were deconvoluted using the Perkin-Elmer Bio Multiview Software.

## Results

**UV–Vis Spectroscopy.** Absorbance spectroscopy was used to monitor changes in the 388 nm Fe–S charge-transfer band of HiPIP upon addition of NO. At pH 7.4, the anaerobic reaction of diethylamine NONOate (DEANO) with reduced native HiPIP was accompanied by a shift in the 388 nm band to 360 nm (Figure 1). A single isosbestic point was observed in the visible region at 379 nm and no further reaction was observed after 30 min using a 20-fold excess of NONOate. A similar result was obtained when an NO-saturated solution was used instead of DEANO. The absorbance of the final product, at 360 nm, was comparable to that of the small-molecule dinitrosyl–iron complex, [(cysteine)<sub>2</sub>Fe(NO)<sub>2</sub>]<sup>–</sup>, which has an absorbance maximum at 358 nm. In addition, NO-inactivated mitochondrial-aconitase, which contains protein-bound DNICs, exhibits a similar optical spectrum to that obtained at the final time point in Figure 1,<sup>13</sup> and so the HiPIP product absorbance was initially assigned to a protein-bound dinitrosyl–iron complex. This was later confirmed by EPR spectroscopy.

The reactions of native and Tyr19Leu HiPIP with various concentrations of NONOate were monitored at 350 nm, the

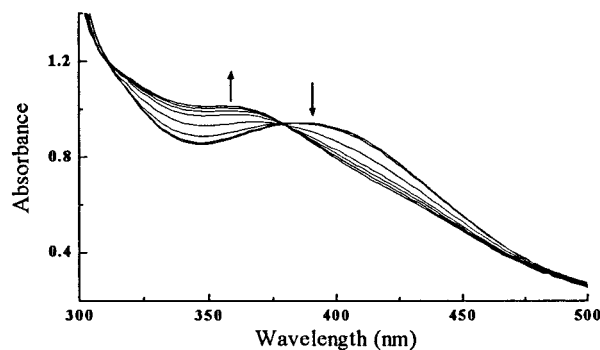


**Figure 1.** UV–vis spectra obtained during the reaction of reduced protein. Timed scans (from 0 to 30 min) for the anaerobic reaction of 50  $\mu\text{M}$  reduced native HiPIP with 1 mM DEANO at room temperature in 50 mM HEPES, pH 7.4.

wavelength at which a maximal change in the UV–vis spectra occurred. Figures 2A and 2B show the results of time-drive experiments for the reaction of reduced native and Tyr19Leu HiPIP, respectively, which were fit to a first-order exponential (Figure 2C). Since NO release from DEANO was time dependent, a minor lag phase was often observed. Varying the concentration of DEANO had an effect on both the rate and the extent of the reaction. In the case of the mutant, although the rate varied approximately linearly with [DEANO], the final amount of cluster degradation was approximately the same following addition of either 5 $\times$  or 20 $\times$  excess NONOate, as judged by the change in absorbance. Although the rates of reaction of native HiPIP also varied linearly with [DEANO], the reactions occurred approximately half as fast relative to the mutant. Furthermore, the rates at 4.5 $\times$  and 6.7 $\times$  excess DEANO were both slower than the rate of NO release (0.08  $\text{min}^{-1}$ ), but with 4.5 $\times$  excess DEANO the amplitude of the absorbance change was found to be  $\sim$ 40% of that for 6.7 $\times$  excess DEANO after 30 min of reaction.

Next, the reaction of oxidized native HiPIP with DEANO was studied in a similar manner. From 0 to 5 min, a rapid decrease in the oxidized spectrum was observed, resulting in a “reduced” species that absorbed at 366 nm (Figure 3A). Based on its absorbance, the “reduced” species was most likely a mixture of both reduced HiPIP (formed via autoreduction) and dinitrosyl–iron-bound product. Autoreduction of HiPIP has previously been observed for hydrolytically unstable mutants.<sup>26</sup> The reducing equivalents for this process presumably come from  $\text{Fe}^{2+}$  and  $\text{S}^{2-}$  released from degraded Fe–S clusters. From 10 to 30 min a shift in absorbance was observed that was similar to that seen for the reduced protein and yielded a product with  $\lambda_{\text{max}} \sim 354$  nm. Time-drive reactions (at 350 nm) of oxidized native and Tyr19Leu HiPIP with a 10-fold excess of DEANO were compared (Figure 3B). Unlike the native protein, the 350 nm absorbance of Tyr19Leu did not change significantly following an initial decrease during the first 10 min of the reaction, suggesting that the mutant protein was completely degraded during this time. The first-order rate constants for the reactions of reduced and oxidized Tyr19Leu HiPIP were 0.30 and 0.36  $\text{min}^{-1}$ , respectively.

**EPR Spectroscopy.** EPR samples were prepared upon reacting native HiPIP with DEANO at pH 7.4 for 60 min. At 15 K, the resulting samples contained a single EPR-active species characteristic of a cysteinyl-coordinated  $d^7$  dinitrosyl–iron complex (Figure 4A) that remained anisotropic at room temperature.<sup>7,13</sup> An identical signal was obtained when Tyr19Leu

(24) Grzesiek, S.; Bax, A. *J. Am. Chem. Soc.* **1993**, *32*, 12593–12594.

(25) Piotto, M.; Saudek, V.; Skelnar, V. *J. Biomol. NMR* **1992**, *2*, 661–666.

(26) Bian, S.; Hille, C. R.; Hemman, C.; Cowan, J. A. *Biochemistry* **1996**, *35*, 14544–14552.

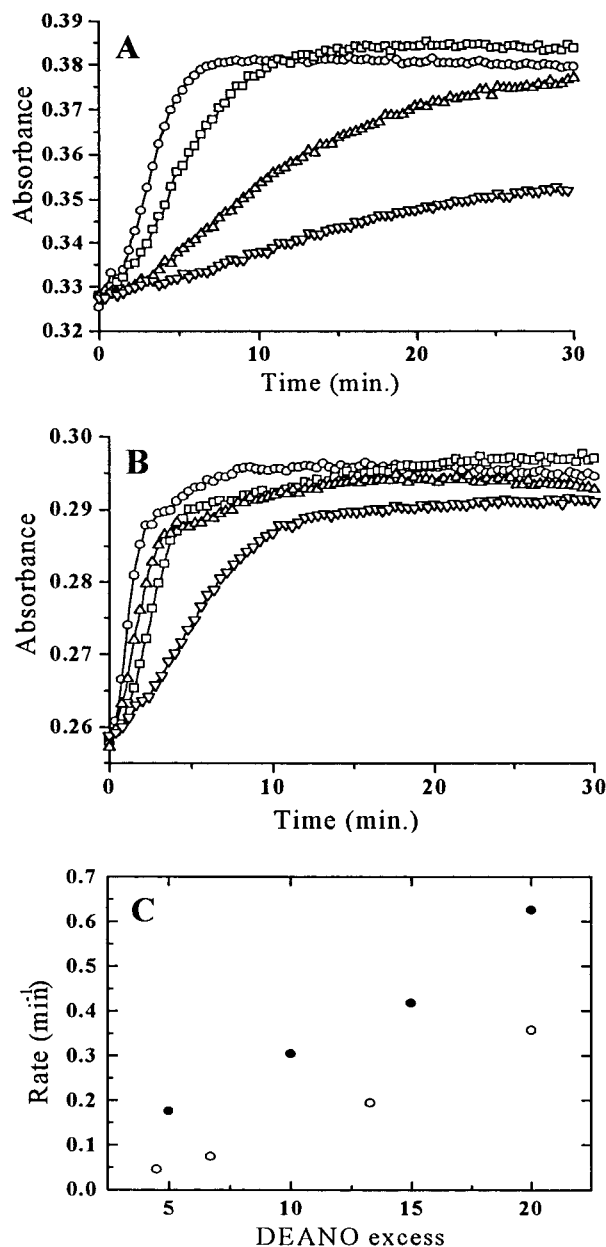


**Figure 2.** Kinetics of reduced Fe-S cluster degradation. UV-vis time drive recorded at 350 nm for the anaerobic reaction of 30  $\mu\text{M}$  HiPIP with DEANO at room temperature in 50 mM Hepes, pH 7.4: (A) native HiPIP + DEANO (20 $\times$ ) (○); + DEANO (13.3 $\times$ ) (□); + DEANO (6.7 $\times$ ) ( $\Delta$ ); + DEANO (4.5 $\times$ ) ( $\nabla$ ). (B) Tyr19Leu HiPIP + DEANO (20 $\times$ ) (○); + DEANO (15 $\times$ ) (□); + DEANO (10 $\times$ ) ( $\Delta$ ); + DEANO (5 $\times$ ) ( $\nabla$ ). (C) Plot of first-order rate constants versus excess of DEANO for native (○) and Tyr19Leu (●) HiPIP.

HiPIP was reacted in a similar manner. In comparison, at 15 K, the synthetic complex,  $[(\text{cysteine})_2\text{Fe}(\text{NO})_2]^-$ , gave a similar axial  $g_{av} = 2.03$  signal that became isotropic at room temperature with hyperfine splitting from both  $^{14}\text{N}$  and the  $\beta$ -methylene protons on cysteine.<sup>7</sup> This demonstrated that the DNIC signal in HiPIP-containing samples was protein bound. Upon addition of an excess of solid dithionite, the  $d^7$  complex was reduced to the corresponding " $d^9$ " dinitrosyl-iron complex (Figure 4B).<sup>13</sup> Furthermore, the intensity of the signal did not change upon evacuation of the sample nor did the oxidized HiPIP signal appear upon subsequent addition of ferricyanide, showing that DNIC formation was irreversible and that the product did not contain the native  $\text{Fe}_4\text{S}_4$  cluster.

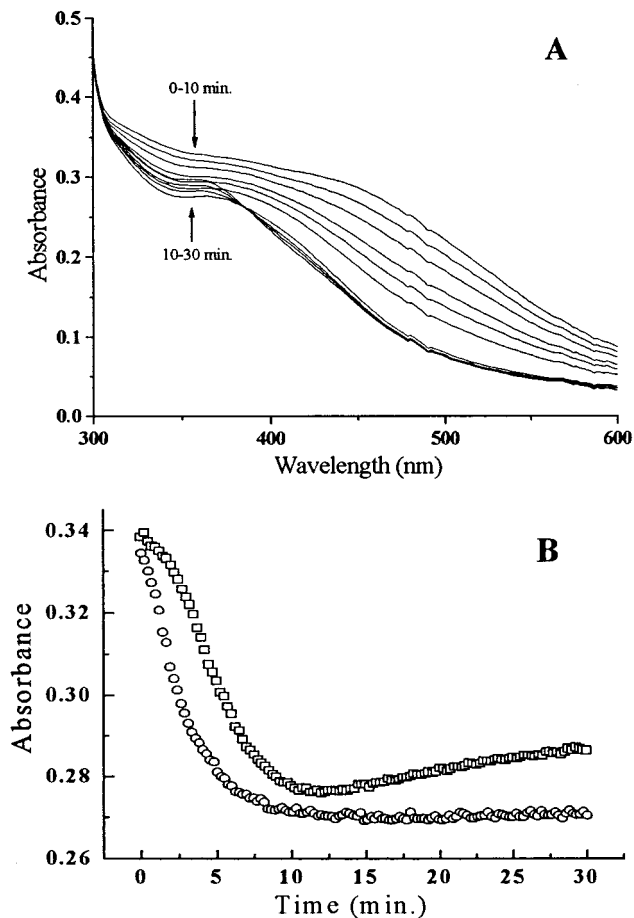


**Figure 3.** UV-vis spectra obtained during the reactions of oxidized HiPIP. (A) Timed scans for the anaerobic reaction of 50  $\mu\text{M}$  oxidized native HiPIP<sub>ox</sub> with 0.5 mM DEANO at room temperature in 50 mM Hepes, pH 7.4. (B) Similar 350 nm time drives for the reaction of 30  $\mu\text{M}$  oxidized native (□) and 30  $\mu\text{M}$  oxidized Tyr19Leu (○) HiPIP with 0.3 mM DEANO.

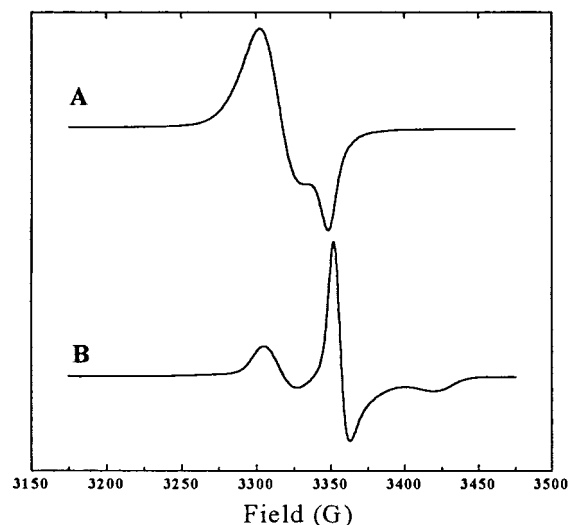


**Figure 4.** EPR spectra of  $d^7$ - and  $d^9$ -DNICs. (A) EPR spectrum obtained after reaction of 1 mM native HiPIP with 20 mM DEANO for 60 min at room temperature in 50 mM Hepes, pH 7.4. (B) EPR spectrum of the sample used in (A) after addition of excess sodium dithionite. Spectra were recorded at 15 K.

The EPR signals in protein-containing samples were integrated to determine the relative extent of DNIC formation for native and mutant proteins. The reaction of reduced native HiPIP and reduced Tyr19Leu HiPIP with DEANO gave DNIC signals



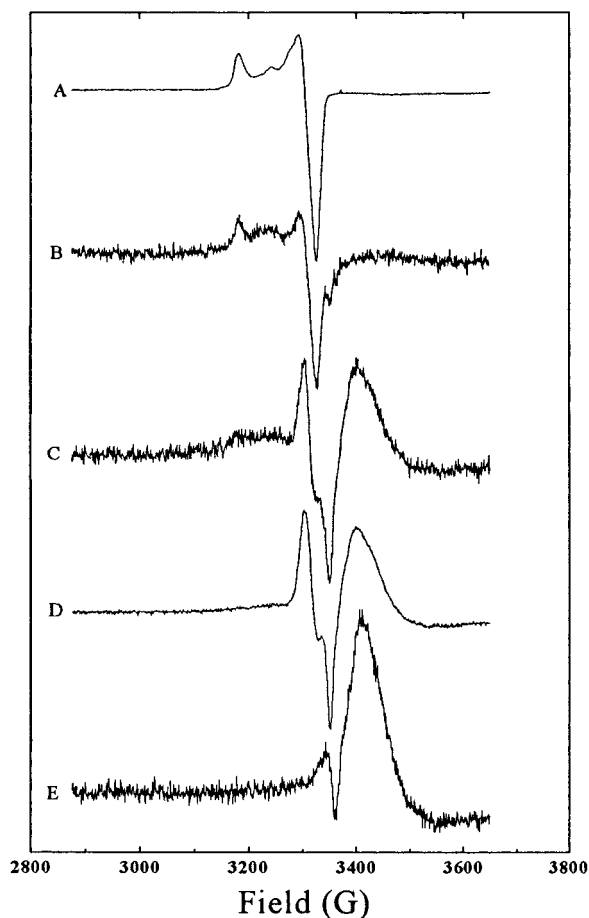


**Figure 5.** Slow freeze-quench EPR spectra. (A) Spectrum of 0.1 mM ferricyanide-oxidized HiPIP. (B) Spectrum obtained after mixing 0.1 mM reduced HiPIP with 2 mM DEANO at room temperature in 50 mM Hepes, pH 7.4, for 15 s prior to freezing in dry ice/acetone. (C and D) Similar to (B) except for a 1 or 5 min delay, respectively, prior to freezing. (E) Spectrum obtained 4 min after mixing 0.3 mM FeSO<sub>4</sub> with 3 mM DEANO at room temperature in 50 mM Hepes, pH 7.4.

that were ~60% and ~35% of the protein concentration, respectively. Since HiPIP contains four cysteines, the signal resulting from dicysteinylnitrosyl-iron species could be at most twice the enzyme concentration. Similar experiments were carried out with ferricyanide-oxidized protein. When oxidized native HiPIP was reacted with DEANO the DNIC signal was ~30% of the enzyme concentration, and when oxidized Tyr19Leu HiPIP was reacted with DEANO (in the presence of excess ferricyanide) the DNIC signal accounted for only ~5% of the protein concentration.

EPR samples were also prepared by flash-freezing solutions of native HiPIP at seconds to minutes after addition of diethylamineNONOate. Although reduced HiPIP ( $S = 0$ ) is EPR silent, the oxidized protein ( $S = 1/2$ ) is EPR active (Figure 5A). After 10–30 s a weak signal from oxidized HiPIP was occasionally observed (Figure 5B). Since protein oxidation was never observed by UV–vis spectroscopy, we expected this to be only a transient intermediate in cluster degradation. After 1 min, the oxidized signal was barely visible, relative to both the  $g_{av} = 2.03$  signal and a broad anisotropic signal observed at  $g < 2.0$  (Figure 5C). At longer times, both the  $g_{av} = 2.03$  and  $g < 2.0$  signals grew more intense, but the oxidized HiPIP signal was no longer visible (Figure 5D). A similar  $g < 2.0$  signal has previously been observed during the reaction of soybean lipoxygenase with NO, and has been ascribed to a high-spin

Fe<sup>2+</sup>–NO complex.<sup>27,28</sup> An identical signal was observed upon addition of DEANO to FeSO<sub>4</sub> (Figure 5E), and so it is postulated that the  $g < 2.0$  signal in Figures 5C and 5D arises from an Fe<sup>2+</sup>–NO species, but is not protein bound.

Finally, we attempted to determine whether a protein-bound DNIC could be synthesized from apo-HiPIP. Thus, apo-HiPIP was reacted with FeSO<sub>4</sub> and DEANO for 1 h and subsequently desalted on a G-25 column. At 15 K, the EPR spectrum of the product containing ~0.2 mM protein gave no observable DNIC signal. If a protein-bound DNIC species was formed, it perhaps accounted for less than a 1% stoichiometry of DNIC to protein.

**NMR Spectroscopy.** <sup>15</sup>N–<sup>1</sup>H HSQC NMR spectroscopy of <sup>15</sup>N-labeled HiPIP has previously been used to observe folding and unfolding of apo and native HiPIP, respectively.<sup>29,30</sup> The HSQC spectrum resulting from the reaction of HiPIP with DEANO or NO gas lacked the dispersion of N–H cross-peaks observed for the native protein.<sup>30</sup> The product spectrum did, however, closely resemble that for apo-HiPIP, and so the protein-bound DNICs do not appear to induce significant structure on the polypeptide. Rather, the protein appears to be unfolded.

**Mass Spectrometry.** Electrospray ionization mass spectrometry (ESI-MS) was used to better characterize the products of NO-mediated degradation. Although DNICs had never been observed by mass spectrometry, ESI-MS has been used to observe protein and heme nitrosylation.<sup>31,32</sup> Since the pI of HiPIP is ~3.7, LC-ESI-MS experiments were run under acidic conditions (0.05% trifluoroacetic acid) to ensure sufficient protonation for positive-ion detection. ESI-MS of native HiPIP under milder conditions in either positive-ion or negative-ion modes has been reported (pH 2.4 and pH 8, respectively);<sup>33</sup> however, under these conditions minor products from NO-mediated degradation were not observed due to insufficient signal to noise. The limitation of this experiment is that apo-HiPIP cannot be distinguished from holo-HiPIP when the sample is subjected to the LC step. Under the conditions of HPLC purification (90% CH<sub>3</sub>CN/0.05% TFA), the acid labile iron–sulfur cluster is lost, and so control samples of native HiPIP give evidence only of a species corresponding to apoprotein, with a mass of 9447 ± 1 Da.

Native HiPIP was reacted with DEANO at pH 7.4 and the products were determined by LC-ESI-MS, giving the mass spectrum shown in Figure 6A. After deconvolution, two sets of major species were observed (Figure 6B), corresponding to apo-HiPIP (**I**: observed mass = 9442 ± 1 Da; calculated mass = 9442 Da assuming the cysteines are not protonated) and apo-HiPIP having two bound DNICs (**III**: observed mass = 9674 ± 1 Da; calculated mass = 9674 Da), but additional peaks that most likely correspond to NO adducts of species **I** and **III** were also observed, separated by 31–33 Da. The relative intensity of **I**, including NO-adducts, was roughly twice that of **III**, including NO adducts, which agreed with EPR spin integrations that indicated a 0.6:1 DNIC:protein stoichiometry. No peak was

(27) Galpin, J. R.; Veldink, G. A.; Vliegthart, J. F. G.; Boldingh, J. *Biochim. Biophys. Acta* **1978**, *536*, 356–362.

(28) Salerno, J. C.; Siedow, J. N. *Biochim. Biophys. Acta* **1979**, *579*, 246–251.

(29) Bertini, I.; Cowan, J. A.; Luchinat, C.; Natarajan, K.; Piccioli, M. *Biochemistry* **1997**, *36*, 9332–9339.

(30) Natarajan, K.; Cowan, J. A. *J. Am. Chem. Soc.* **1997**, *119*, 4082–4083.

(31) Mirza, U. A.; Chait, B. T.; Lander, H. M. *J. Biol. Chem.* **1995**, *270*, 17185–17188.

(32) Upmacis, R. K.; Hajjar, D. P.; Chait, B. T.; Mirza, U. A. *J. Am. Chem. Soc.* **1997**, *119*, 10424–10429.

(33) Petillot, Y.; Forest, E.; Meyer, J.; Moulis, J.-M. *Anal. Biochem.* **1995**, *228*, 56–63.

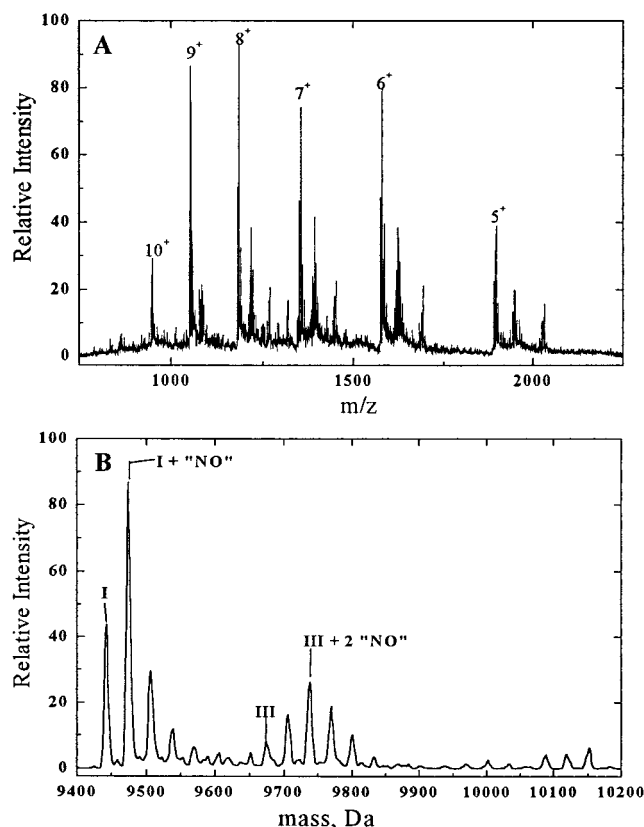


**Figure 6.** LC-ESI-MS spectrum of protein-bound DNICs. (A) Mass spectrum and (B) reconstructed mass spectrum for reaction of 1 mM native HiPIP<sub>red</sub> with 20 mM DEANO at room temperature in 50 mM Hepes, pH 7.4, followed by desalting on a G-25 column.

observed at 9558 Da—the mass that would correspond to **I** (apo-HiPIP with one DNIC). Higher molecular mass species were observed but have not been identified. While the relative peak intensities of the observed products may not quantitatively correlate with their actual abundance, nevertheless, the pattern of nitrosylation was distinct for **I** vs **III**. Overall, the apo-HiPIP species **I** had an average of  $\sim 1.2$  “NO’s” per protein, and the apo-HiPIP-(DNIC)<sub>2</sub> species **III** had an average of  $\sim 2.2$  “NO’s” per protein. Other peaks were barely visible above the baseline and comprised  $< 1\%$  of the total protein; whereas **III** comprised one-third of the total protein.

Apo-HiPIP was also reacted with DEANO to observe the extent of nitrosation/nitrosylation in the absence of the iron-sulfur cluster. Two major species and their corresponding NO adducts were observed (data not shown). Apo-HiPIP ( $9442 \pm 1$  Da) was most abundant, but an additional species was observed at 9424 Da that was possibly a product of dehydration formed during preparation of apo-HiPIP. Nonetheless, the relative abundance of the apo-HiPIP species with 0 to 3 “NO’s” was 1:0.5:0.15:0.07, and the average number of “NO’s” was 0.6 per protein, half as much as was observed for **I** (Figure 6B).

## Discussion

We have studied the reaction of nitric oxide with HiPIP to better understand the principles governing the reactivity of NO with iron-sulfur proteins and the biological consequences of such reactions. To this end, our objectives are 3-fold: to characterize the products of the reaction between NO and HiPIP; to understand the mechanisms of cluster degradation and DNIC formation; and to elucidate the general factors that control the

reactivity of NO with protein-bound Fe-S centers. These issues are now discussed.

**Characterization of Reaction Products.** EPR has long been the standard technique for identifying protein-bound dinitrosyl-iron clusters.<sup>7,8,11</sup> As such, it can be used to identify the nature of the coordinating ligands to iron and to quantitate the number of protein-bound DNICs, but not to determine their precise stoichiometry. In this study, EPR results show that NO-mediated degradation of native HiPIP results in the formation of protein-bound DNICs with an average stoichiometry of around 0.6 DNICs per protein. The nature of the EPR signal demonstrates that these dinitrosyl-iron complexes are ligated to two cysteines rather than being of mixed ligand coordination; for example, coordination to histidine and cysteine would give rise to a rhombic rather than an axial  $g_{av} = 2.03$  signal.<sup>5</sup>

ESI-MS represents a novel technique for observing protein-bound DNICs, and we have observed such species directly for the first time. More importantly, ESI-MS can be used to determine the stoichiometry of protein-bound DNICs, and our results show that the dinitrosyl-iron complexes are found with a 2:1 ratio of DNIC to protein in roughly one-third of the total protein.

Adducts of apo-HiPIP (**I**) and (DNIC)<sub>2</sub>-HiPIP (**III**) that result from chemical modification of the protein by nitric oxide are also observed by ESI-MS, although our data do not identify the precise chemical nature of these adducts. With mass differences of 31–33 Da, these products may include nitrosamides and nitrosamines (N-NO, +29 Da), cysteine sulfinic acid (Cys-SO<sub>2</sub>H, +32 Da), and S-nitrosocysteine (Cys-S-NO, +30 Da).<sup>20,34,35</sup> However, HiPIP contains only four cysteine residues, which in **III** are all coordinated to DNICs, and therefore these adducts cannot be nitrosothiols, but are most likely nitrosamines derived from an amine-containing side chain (Lys, Arg, His, Trp) or the N-terminal amine. As far as we know, this is the first evidence for nitrosation of an iron-sulfur protein in response to cluster degradation by NO.

Since apo-HiPIP has four uncoordinated cysteines, we would expect **I** to have on average a greater number of NO adducts than **III**, especially in light of reports that thiols are more reactive toward NO than amines.<sup>35</sup> That this is not the case suggests either that the cysteines are involved in disulfide bonds (vide infra) or that S-nitrosylation does not occur under our experimental conditions. Two previous reports that characterize peptide and protein nitrosylation by ESI-MS have demonstrated the sensitivity of the S-NO bond, in particular, to homolysis under certain experimental conditions.<sup>31,32</sup> Accordingly, it is also possible that the S-nitrosothiols do form but are labile under the conditions of the LC-ESI-MS experiment.

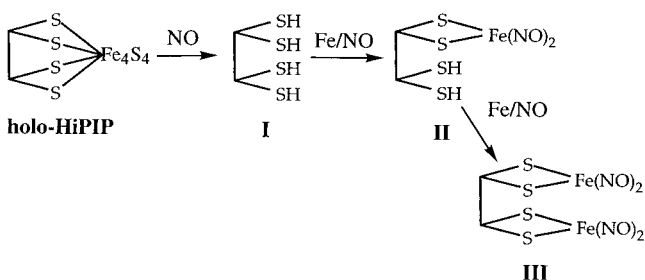
**Cluster Degradation and DNIC Formation.** The stoichiometry of DNIC to protein, as determined by ESI-MS, suggests a correlation between the mechanism of cluster degradation and the distribution of protein-bound DNICs. It is well established that apo-HiPIP has little or no secondary or tertiary structure relative to the holoprotein,<sup>36</sup> and so, if HiPIP reacts with NO to give an apoprotein that is then capable of forming two protein-bound dinitrosyl-iron clusters, we would anticipate a stepwise formation of the protein-bound metal complexes (Scheme 1) to yield a mixture of **I**, **II**, and **III**. However, ESI-MS results show that protein species have either none or two DNICs, suggesting a mechanism by which both formation of **III** is rapid,

(34) Becker, K.; Savvides, S. N.; Keese, M.; Schirmer, R. H.; Karplus, P. A. *Nat. Struct. Biol.* **1998**, *5*, 267–271.

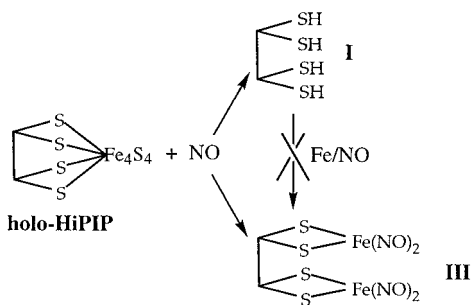
(35) Simon, D. I.; Mullins, M. E.; Jia, L.; Gaston, B.; Singel, D. J.; Stamler, J. S. *Proc. Natl. Acad. Sci. U.S.A.* **1996**, *93*, 4736–4741.

(36) Cowan, J. A.; Lui, S. M. *Adv. Inorg. Chem.* **1998**, *45*, 313–350.

## Scheme 1



## Scheme 2



such that **II** is not observed, and the cysteines of **I** are inactivated toward DNIC formation, such that **I** cannot form (**II** or **III**) (Scheme 2).

Inhibition of DNIC formation need not occur via chemical modification of the cysteines, but could be a result of spatial separation of these residues following protein unfolding. We have shown by EPR that DNICs are not formed upon reaction of apo-HiPIP with excess Fe(II) and DEANO. On the other hand, addition of excess NO(g) to cysteine and FeSO<sub>4</sub> gives a >98% yield of [(Cys)<sub>2</sub>Fe(NO)<sub>2</sub>].<sup>3</sup> In the case of small-molecule DNIC formation, the proximity of the cysteinyl thiolate ligands is not restricted inasmuch as the free ligands are not held at fixed distances from one another in solution. This suggests a mechanism by which formation of **III** is concerted with cluster degradation while the protein remains essentially folded. By the same argument, assuming no chemical modification of the cysteines, formation of **I** is expected when protein unfolding occurs prior to DNIC formation.

Under anaerobic conditions, we expect that nitric oxide, and not higher-order NO<sub>x</sub> species,<sup>37</sup> causes cluster degradation. Inasmuch as the oxidation potential of HiPIP<sup>(2+/3+)</sup> is +0.35 V,<sup>2,36</sup> one would predict that NO, with a reduction potential of +0.38 V,<sup>1,2</sup> should oxidize the Fe<sub>4</sub>S<sub>4</sub> cluster. However, it is apparent from UV–vis and EPR data that oxidation is not rapid. Although a weak and presumably transient oxidized signal is observed by EPR, this species need not be an obligatory intermediate in cluster degradation. It is likely that the first step in cluster degradation is attack by nitric oxide at either an iron or sulfur center of the cluster.

If the determining step for formation of **I** is protein unfolding, this suggests that the cluster is first nitrosylated, with NO displacing one or more cysteine ligands. Since there is a strong correlation between protein structure and cysteine coordination, ligand displacement might cause local unfolding of the protein structure to allow solvolysis of the nitrosylated cluster. Furthermore, since the protein begins to unfold with concomitant cluster degradation, the resultant product will consist of apo-protein, which will be inactive toward DNIC formation. For

this mechanism to compete with the alternative, inactivation must occur faster than DNIC formation. By contrast, we anticipate that formation of **III** occurs via rapid degradation of the iron–sulfur cluster by NO without a prerequisite hydrolysis step. In this way the protein will be folded and the cysteines will lie in close proximity such that DNIC formation is facile.

**Factors Governing NO Reactivity.** NO(g) must attack the Fe–S cluster either by diffusion through the protein or by diffusion through solvent that is accessible to the cluster. In earlier studies we have shown that the Fe<sub>4</sub>S<sub>4</sub> cluster of native HiPIP is solvent inaccessible, as defined by the rate of solvent exchange of backbone amide protons, thereby preventing hydrolytic instability of the oxidized cluster.<sup>36</sup> Mutation of the structurally conserved Tyr-19, however, increases the solvent accessibility of the cluster, resulting in rapid hydrolysis of the oxidized cluster.<sup>22,38</sup> While solvent accessibility, as defined, is not an absolute requirement for NO-mediated cluster degradation, it is clear that complete degradation of the mutant requires a smaller excess of DEANO and occurs at a faster rate than for native HiPIP (Figure 2). Furthermore, EPR spin integration shows that degradation of the mutant protein results in the formation of fewer DNICs. Since there is little difference between Tyr19Leu and native HiPIP, other than solvent accessibility, this is an obvious factor for explaining the differences in reactivity. Formation of **I** and **III** both require NO, and so an increase in the solvent accessibility should increase the effective NO concentration at the cluster, causing an enhancement in the overall rate of degradation. Likewise, if formation of **I** occurs via a hydrolytic mechanism, we would expect an increase in the solvent accessibility to effect an increase in the formation of **I**, relative to **III**, as observed.

Since autoreduction is a component of the reaction of oxidized HiPIP with NO, it is difficult to compare rates of reactivity between reduced and oxidized clusters. Qualitatively, however, oxidized HiPIP reacts with NO at a faster rate than reduced HiPIP, and we have shown by EPR that fewer DNICs are formed upon reaction of oxidized HiPIP as compared to reduced HiPIP. Generally, NO interacts more strongly with ferrous ion than with ferric iron, since Fe<sup>2+</sup> has an additional d-electron for back-bonding.<sup>1,2</sup> Similarly, the reaction of NO with the more electrophilic oxidized cluster [Fe<sub>4</sub>S<sub>4</sub>]<sup>3+</sup> is likely to occur more slowly than with the reduced cluster [Fe<sub>4</sub>S<sub>4</sub>]<sup>2+</sup>. However, the oxidized cluster is significantly more prone to solvolysis than the reduced cluster, and so after the initial attack by NO, hydrolysis of the oxidized, nitrosylated cluster should be more rapid, accounting for the observed increase in formation of **I**.

The reactions of nitric oxide with a variety of 2Fe-2S and 4Fe-4S proteins are now well documented. Although members of both of these classes of proteins (2Fe-2S = SoxR,<sup>39</sup> mammalian ferrochelatase;<sup>40</sup> 4Fe-4S = m- and c-aconitase,<sup>13</sup> *C. botulinum* Fd,<sup>8</sup> HiPIP (this work), and mitochondrial complexes I and II<sup>10,41</sup>) form DNICs upon reaction with NO, a number of these proteins show differential sensitivity toward NO.<sup>13</sup> Furthermore, spinach ferredoxin (2Fe-2S) and the Rieske 2Fe-2S cluster of mitochondrial complex III are not degraded under conditions where other 2Fe-2S and 4Fe-4S clusters are observed to form DNICs.<sup>10,40,41</sup> It is unlikely that a high midpoint potential (+300 mV) is responsible for the resistance of the

(38) Li, D.; Agarwal, A.; Cowan, J. A. *Inorg. Chem.* **1996**, *35*, 1121–1125.

(39) Hidalgo, E.; Bollinger, J. M.; Bradley, T. M.; Walsh, C. T.; Demple, B. *J. Biol. Chem.* **1995**, *270*, 20908–20914.

(40) Sellers, V. M.; Johnson, M. K.; Dailey, H. A. *Biochemistry* **1996**, *35*, 2699–2704.

(41) Welter, R.; Yu, L.; Yu, C.-A. *Arch. Biochem. Biophys.* **1996**, *331*, 9–14.

(37) Cornforth, D. In *Nitric Oxide: Principles and Actions*; Lancaster, J., Ed.; Academic Press: San Diego, CA, 1996; pp 259–287.



Rieske cluster, since HiPIP has an even higher  $E_m$  (+350 mV). Our results indicate that solvent accessibility can play an important role in determining cluster reactivity toward NO, but cannot address the dependence on ligand type (i.e., Cys vs His).

**Nitrosylation Reactions.** As stated before, we presume that under anaerobic conditions, and at physiological pH, nitric oxide will be the predominant reactive species. However, NO alone is not known to cause protein nitrosation, and so there are several explanations for the NO adducts observed by ESI-MS. First, the presence of trace oxygen or metal contaminants could promote protein nitrosation/nitrosylation via formation of  $\text{NO}_x$  species or  $\text{NO}^+$ .<sup>34,42</sup> Alternatively, transnitrosation may occur, whereby amines attack DEANO directly, essentially making the NONOate an  $\text{NO}^+$  donor.<sup>1</sup> It is most likely that the nitrosation observed upon degradation of native HiPIP (Figure 6B) is catalyzed either by  $\text{NO}^+$  formed from the reaction of NO with free iron released from degraded cluster or by similarly reactive  $\text{Fe/NO}/(\text{S}^{2-})$  complexes.<sup>37</sup> Although some nitrosation of apo-HiPIP is observed when the protein is reacted with DEANO, it does not compare with the significant nitrosation observed upon degradation of the holoprotein by NO. The observed nitrosation of apo-HiPIP,  $\sim 0.6$  "NO's" per protein, is most likely the result of trace dioxygen or metals.

We have not yet specifically addressed the possibility that chemical modification of cysteine residues inhibits DNIC formation. Like amines, cysteine can also be nitrosylated by reaction with  $\text{NO}^+$ , while the presence of a proximal cysteine residue can catalyze disulfide bond formation via a transnitrosation mechanism.<sup>1</sup> Mirza et al. have used ESI-MS to demonstrate that at pH 7.8 the reaction of NO with a model peptide containing a single cysteine residue resulted in dimerization of the peptide,<sup>31</sup> presumably via such a transnitrosation mechanism. Thus, either nitrosylation of cysteine residues and/or disulfide bond formation may be responsible for inhibiting DNIC formation.

**Conclusions and Physiological Relevance.** In this study, we have shown that iron–sulfur cluster degradation by nitric oxide not only results in formation of dinitrosyl–iron clusters but also causes significant protein nitrosation. For the first time, protein-bound DNICs have been observed directly by use of ESI-MS, and the stoichiometry of DNIC to protein has been determined. Our data suggest that DNIC formation is intimately related to the mechanism of cluster degradation. Mass spectrometry has

also shown that NO-mediated degradation of an iron–sulfur protein can result in nitrosation of noncysteinyll residues or backbone (presumably forming nitrosamines).

Importantly, we have shown that there is a direct correlation between the solvent accessibility of a biological iron–sulfur cluster and its reactivity with NO and that enhanced solvent accessibility provides a discriminatory mechanism for targeting Fe–S centers at low physiological concentrations of nitric oxide. In particular, when the solvent accessibility of an iron–sulfur cluster is increased, its reactivity with nitric oxide also increases. This issue of solvent accessibility should be very important to the reactivity of proteins with NO in vivo. Not only are the cellular concentrations of NO(g) low, but there has to be a mechanism by which a regulatory pathway involving nitric oxide can be discriminated from the random action of NO. Thus it would be to the advantage of a cytosolic protein, such as the IRP1, to react with NO at concentrations that do not inhibit other cytosolic Fe–S proteins. Our studies of native and Tyr19Leu HiPIP suggest that the IRP1, which has a solvent-accessible iron–sulfur cluster, would require a smaller excess of NO in vivo to effect cluster degradation than would a similar protein having a solvent inaccessible cluster.

Finally, we note that we have used a bacterial HiPIP as a model for more physiologically relevant proteins since the combination of low molecular mass, high expression levels, facility of isotopic labeling, availability of mutants of well-defined solvent accessibility, and facile application of detailed spectroscopic analysis provides a superior level of insight on factors influencing NO chemistry with Fe–S cores relative to, for example, aconitase ( $\sim 10$  kDa vs  $\sim 100$  kDa). We expect that the nitric oxide chemistry of HiPIP, as it relates to the factors controlling cluster degradation, DNIC formation, and protein nitrosation, will be comparable in vitro and in vivo to that of other biologically relevant iron–sulfur proteins.

**Acknowledgment.** We thank Zhaoyang Li at the Ohio State University Campus Chemical Instrument Center for running LC-ESI-MS samples and Craig Hemann and Dr. Russ Hille for acquiring EPR spectra. This work was supported by the Petroleum Research Fund (administered by the American Chemical Society), and by the National Science Foundation (CHE-9706904). J.A.C. is a Camille Dreyfus Teacher-Scholar (1994–99). M.W.F. is supported by the NIH Chemistry and Biology Interface Training Program at Ohio State (GM08512-03).

JA9901056

(42) Chan, N.-L.; Rogers, P. H.; Arnone, A. *Biochemistry* **1998**, *37*, 16459–16464.